Single-hole pump in germanium

Alessandro Rossi[1,2,*] , **Nico W Hendrickx**[3], **Amir Sammak**[4], **Menno Veldhorst**[3],
Giordano Scappucci[3] **and Masaya Kataoka**[2]

[1] Department of Physics, SUPA, University of Strathclyde, Glasgow G4 0NG, United Kingdom
[2] National Physical Laboratory, Hampton Road, Teddington TW11 0LW, United Kingdom
[3] QuTech and Kavli Institute of Nanoscience, Delft University of Technology, Delft, The Netherlands
[4] QuTech and Netherlands Organisation for Applied Scientific Research (TNO), Delft, The Netherlands

E-mail: alessandro.rossi@strath.ac.uk

CrossMark

Abstract
Single-charge pumps are the main candidates for quantum-based standards of the unit ampere
because they can generate accurate and quantized electric currents. In order to approach the
metrological requirements in terms of both accuracy and speed of operation, in the past decade
there has been a focus on semiconductor-based devices. The use of a variety of semiconductor
materials enables the universality of charge pump devices to be tested, a highly desirable
demonstration for metrology, with GaAs and Si pumps at the forefront of these tests. Here, we
show that pumping can be achieved in a yet unexplored semiconductor, i.e. germanium.
We realise a single-hole pump with a tunable-barrier quantum dot electrostatically defined at a
Ge/SiGe heterostructure interface. We observe quantized current plateaux by driving the system
with a single sinusoidal drive up to a frequency of 100 MHz. The operation of the prototype was
affected by accidental formation of multiple dots, probably due to disorder potential,
and random charge fluctuations. We suggest straightforward refinements of the fabrication
process to improve pump characteristics in future experiments.

Keywords: single-hole pump, germanium, quantum metrology, quantum dot

(Some figures may appear in colour only in the online journal)

1. Introduction

A single-charge pump is an electronic device that can generate quantized electric current by clocking the transfer of individual charged quasi-particles (electrons, holes or cooper pairs) with an external periodic drive [1]. The pumped current can be expressed as $I = nef$, where e is the elementary charge, f is the frequency of the drive and n is an integer representing the number of particles transferred per period. The development of this technology has been mainly motivated by its possible application for quantum-based standards of electric current [2]. To date, the most promising pump realisations are semiconductor quantum dots (QDs) with tunable tunnel barriers [3–6], which have demonstrated to operate at the highest frequencies (up to few GHz) with the lowest current uncertainty (below part per million), in the pursuit of meeting the stringent metrological requirements [7].

At the core of the any quantum standard lies the concept of universality. This is the idea that the operation of the standard is based on fundamental principles of nature, rather than being dependent on its specific physical implementation. For example, the acceptance of the Quantum Hall Effect as a primary standard of resistance was driven by the experimental demonstrations of agreement at a level of relative uncertainty below 10^{-10} among Hall devices manufactured in silicon and GaAs, and later in graphene [8, 9]. Similarly, universality expects that the quantised currents generated by singe-charge pumps do not depend on the material system used. Recently, a study of this kind has shown that there is agreement at a level of

---

J. Phys. D: Appl. Phys. **54** (2021) 434001

A Rossi *et al*

$\approx 10^{-6}$ between silicon and GaAs pumps [4], an encouraging stepping stone for future tests with higher accuracy. Hence, from a universality standpoint, it is of interest to investigate a range of material and device systems that can support clocked charge transfers. In fact, besides the advanced performance achieved with QD pumps, there have been other less fulfilling demonstrations in superconductors [10, 11], normal metal [12], hybrid normal/superconductive metal [13], single atoms [14, 15], and graphene [16].

Here, we introduce a new material system to the family of single-charge pumps, i.e. germanium (Ge). We demonstrate single-hole transfers clocked by a single sinusoidal drive in a tunable-barrier QD electrostatically formed at a Ge/SiGe heterostructure interface. We ascertain that the value of the current plateaux scales linearly with the rf drive frequency up to 100 MHz, as expected for quantized transport. We observe unusual plateaux boundaries in the 2D pump maps and tentatively attribute them to multiple parallel pump operation. We also observe device instability due to random charge fluctuations and suggest changes in the fabrication of the next generation of pumps that may mitigate this problem.

2. Methods

The sample used in the experiments was fabricated on a Ge/SiGe heterostructure grown on a 100 mm n-type Si(001) wafer [17]. The material stack is composed of a 16 nm thick compressively strained Ge quantum well grown on a strain-relaxed $Si_{0.2}Ge_{0.8}$ buffer layer. The Ge quantum well (QW) is undoped and separated from the semiconductor/oxide interface by a 22 nm $Si_{0.2}Ge_{0.8}$ barrier, as shown in figure 1(a). A two-dimensional hole gas with densities up to 6×10^{11} cm^{-2}, transport mobility up to 5×10^5 cm^2 Vs^{-1}, and effective mass of $\approx 0.05\ m_e$, where m_e is the free electron mass, is accumulated in the Ge QW via electrostatic gating [18]. The device's gate layout is shown in figure 1(b). Ohmic contacts (shown in green) are defined by electron beam lithography, electron beam evaporation and lift-off of a 30-nm-thick Al layer. Electrostatic gates consist of two Ti/Pd layers with thickness of 20 nm and 40 nm for the barrier (red) and plunger gate (magenta) layer, respectively. Both layers are separated from the substrate and each other by 10 nm of ALD-grown Al_2O_3 [19].

The measurement set-up is schematically represented in figure 1(b). The metal gates are connected to programmable dc voltage sources through room-temperature low-pass filters (not shown). The gate voltages are used to selectively accumulate holes in the Ge QW, resulting in the formation of tunnel barriers (under gates B_{in} and B_{out}) that separate a quantum dot (under PL) from the hole reservoirs. Note that one remaining gate is kept at ground potential at all times to laterally confine the QD in the orthogonal direction to transport. The device current, I, is measured by a low-noise transimpedance amplifier connected to an ohmic contact. Gate B_{in} is connected to an rf source through a low-temperature bias-tee. This gate operates as the entrance barrier for the pumping cycle by clocking the

loading of holes into the QD. The pumping protocol used in this work is known as the ratchet mode, which typically applies to single-QD single-drive pumps and is largely insensitive to device bias [20]. Each pumping cycle begins with the rf drive rising the potential of the entrance barrier loading the QD with holes from the nearest reservoir. Then the rf drive lowers the barrier to trap holes and eject them across the exit barrier, B_{out}, and onto the other reservoir, as depicted in figure 1(c). Unless otherwise stated, the measurements presented in this work are carried out with only a small stray bias across device ohmics due to the amplifier ($V_{bias} \approx 250\ \mu$V), no intended bias voltage is otherwise applied during pumping. The sample is cooled in a cryogen-free dilution refrigerator with a base temperature of approximately 12 mK, although the effective device temperature may be higher due to heating generated by the rf drive.

3. Results

In order to tune the device into a single-QD operation regime, the transconductance is measured as a function of dc voltages applied to both barriers with the rf source turned off. As illustrated in figure 1(d), for a fixed $V_{PL} = -1.2$ V, parallel coulomb blockade peaks appear diagonally across the studied parameter space, a clear indication of single QD formation [21]. For less negative values of V_{PL}, honeycomb-like stability diagrams are observed (not shown), suggesting a double QD regime possibly due to a parasitic dot created by disorder potential. This informed the decision of carrying out ratchet experiments at $V_{PL} < -1.2$ V. As highlighted by the dashed lines in panel (d), on occasions the coulomb peaks present abrupt discontinuities. This fact is an indication that random charge rearrangements are occurring in or in the vicinity of the QD, resulting in discrete jumps in the current level at a given operation point. It is likely that charge traps at the interface between different layers of the material stack may be responsible for this effect. Four (nominally identical) devices have been tested, and they have all showed roughly the same level of random fluctuations in d.c. tests.

By applying a sinusoidal drive to the entrance gate with peak-to-peak voltage at the 50Ω output of the source $V_{pp} = 0.275$ V, a current plateau at $I = ef$ emerges, as shown in figure 2. For lower values of V_{pp} a current plateau is not observed. In fact, a strong capacitive coupling between the entrance gate and the QD in combination with a sufficiently large rf modulation provides captured holes with the energy shift needed to pass below the exit barrier and eventually be emitted at the end of a pump cycle [22], similarly to a previous report of silicon single-hole pumping [23]. In figure 2(a), one can note the effect of the mentioned random fluctuations. The onset of the plateau region with respect to V_{Bout}, the so-called capture line, is expected to be linearly dependent on V_{Bin} as merely dictated by capacitive coupling considerations [20]. By contrast, in our data this is not discernible because the plateau undergoes discrete random shifts at every voltage scan. By performing measurements at different frequencies we confirm that the pumped current scales as expected for a single
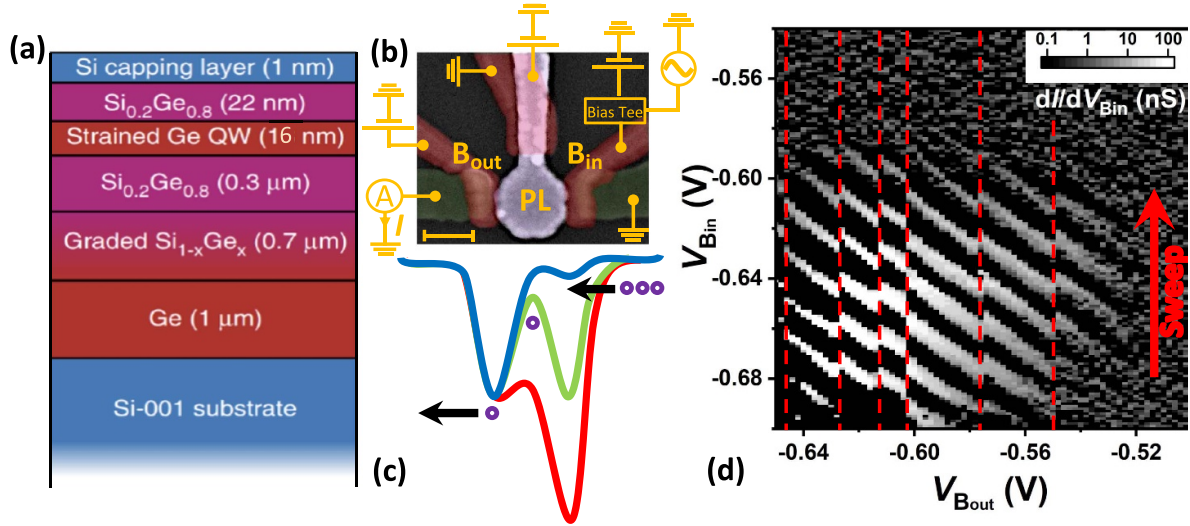
J. Phys. D: Appl. Phys. **54** (2021) 434001

A Rossi *et al*

Figure 1. (a) Schematic depiction of the Ge/SiGe heterostructure stack. (b) SEM image of the device gate layout and schematic of the experimental set-up. Different metallization layers are color coded: Al (green), Ti/Pd layer 1 (red), Ti/Pd layer 2 (magenta). Scale bar represents 100 nm. (c) Valence band energy profile during a pumping cycle: loading (blue), trapping (green), ejection (red). Holes are represented by empty circles. (d) Device transconductance as a function of V_{Bout} and V_{Bin} for $V_{PL} = -1.2$ V and $V_{bias} = 1$ mV. Red dashed lines are guides to the eye to highlight random switching events. The vertical arrow shows the direction of the voltage sweeps.
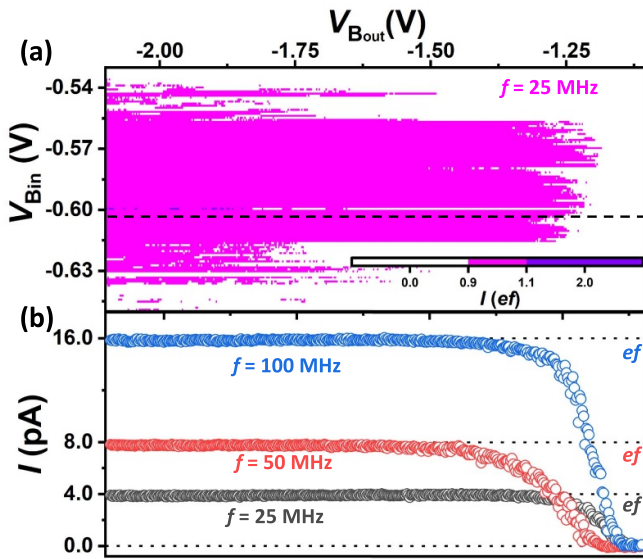

Figure 2. (a) Pumped current as a function of entrance and exit barrier gate voltages at $f = 25$ MHz. Black dashed line is a guide for the eye to indicate the region of parameter space of panel (b). The other experimental parameters are $V_{PL} = -1.40$ V, $V_{pp} = 0.275$ V. (b) Pumped current as a function of V_{Bout} at $f = 25$ MHz (black circles), $f = 50$ MHz (red), $f = 100$ MHz (blue). Other experimental parameters are $V_{pp} = 0.275$ V and $V_{Bin} = -0.602$ V. Black dotted lines indicate the current values expected for quantized pumping, $I = ef$, at the drive frequencies used in the experiment.

hole transported per clock cycle, as reported in figure 2(b). It is of note that in these measurements the current is not seen to increase towards $I = 2ef$, as one would expect for increasingly negative exit barrier voltage, which would normally allow to trap and emit an additional hole. This may be due to a large

charging energy in the QD, which prevents additional holes from being trapped, or insufficient amplitude of the rf drive resulting in incomplete emission [20].

In order to test the latter hypothesis, we have increased the drive amplitude to $V_{pp} = 0.3$ V. However, this resulted in a severe worsening of the charge fluctuations and did not allow a conclusive test to be carried out. In order to modify the QD charging energy, a pump map is acquired at a more negative V_{PL}, see figure 3(a). This is expected to have the main effect of reducing the QD charging energy by enhancing its electrostatically-defined size. A secondary effect is the enhancement of both barriers transparency due to cross-coupling. The map shows that in these circumstances the current rises above the first plateau value for increasingly negative V_{Bout}, albeit without fully reaching the second plateau.

The shape of the current staircase between two adjacent plateaux as a function of the exit barrier gate voltage can provide insights into the process by which the QD is decoupled from the reservoir(s) [20], as indicated by the theoretical fits reported in figure 3(b). Thus far, most of accurate semiconductor pumps [4] have operated in the decay cascade regime [22], where the final number of charged particles in the QD is determined by a one-way cascade of back-tunneling events. According to this model, the average number of holes captured per cycle can be written as

$$\langle n \rangle = \sum_m \exp[-\exp(-\alpha V_{Bout} + \Delta_m)] \qquad (1)$$

where α and Δ_m are fitting parameters. Alternatively, if the reservoir in the vicinity of the entrance gate is heated by the large-amplitude ac drive, charge capture may follow a thermal equilibrium regime. This operation mode has been previously observed in both electron and hole pumps in silicon [3, 23]. In
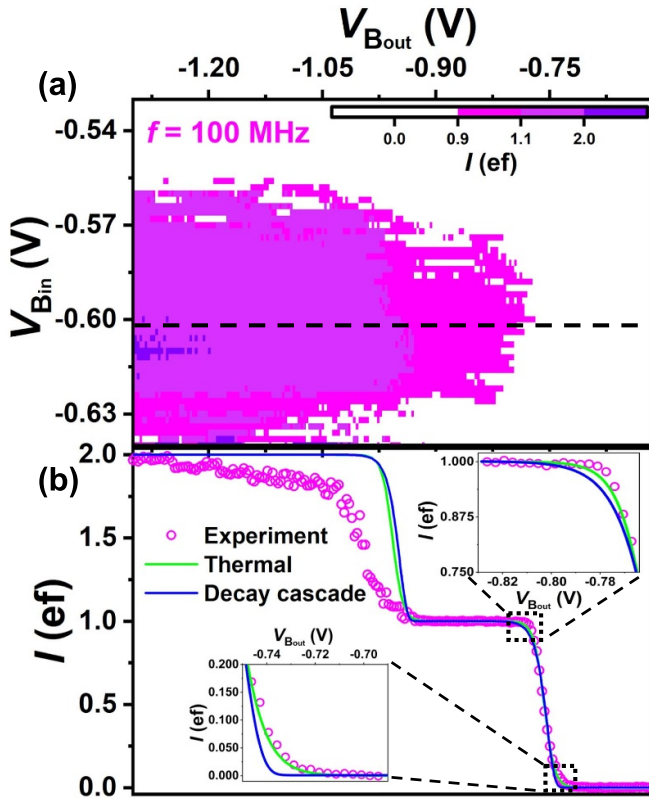
Figure 3. (a) Pumped current as a function of entrance and exit barrier gate voltages at $f = 100$ MHz. Black dashed line is a guide for the eye to indicate the region of parameter space of panel (b). The other experimental parameters are $V_{pp} = 0.275$ V, $V_{PL} = -1.42$ V. (b) Measurements of pumped current as a function of V_{Bout} (circles) and fits to theoretical models (solid lines) for $V_{Bin} = -0.601$ V. Other experimental parameters as in panel (a). Insets: selected data from the main panel on exploded scales to closely compare the goodness of the fits.

this regime, particles are exchanged between the QD and the leads only during the initial stage of the pumping cycle, and the average number of captured holes can be written as [24]

$$\langle n \rangle = \sum_m \frac{1}{1 + \exp(A_m + BV_{Bout})} \quad (2)$$

where A_m and B are the fitting parameters for the *m*th current plateau. In figure 3(b), the normalized pumped current, *I/ef*, is used in the numerical fit of $\langle n \rangle$ for both decay-cascade and thermal models in the range -0.95 V $< V_{Bout} < -0.60$ V. A close inspection of the current staircase (see insets) shows that the thermal equilibrium model is a better fit than the decay cascade for the rising edge approaching $\langle n \rangle = 1$. The fitting error for the thermal model, reduced-$\chi^2_{th} = 0.13$, is significantly lower than for the decay cascade model, reduced-$\chi^2_{decay} = 0.85$, for $V_{Bin} = -0.601$ V. Similar results are obtained by fitting traces at other V_{Bin} values (not shown). This suggests that this hole pump operates in the thermal regime. However, it is clear that the rising edge to the second plateau is not well represented by either model. This is not unusual and it may be an indication that also other phenomena affect the pumping process, which may include a change

in gate coupling between single- and multi-particle QD configurations [25], as well as the presence of additional pumping entities such as traps or parasitic states besides the intended QD [26, 27].

In order to investigate this aspect, pump maps showing multiple plateaux have been acquired under different experimental conditions, as shown in figure 4. Maps in (a) and (b) are taken for different values of V_{PL} and both present current plateaux for $\langle n \rangle = 1$ and $\langle n \rangle = 2$ in a similar fashion to what is already shown in figure 3(a). By contrast, the map in figure 4(c) presents higher current values approaching $\langle n \rangle = 3$ in addition to lower order plateaux. This measurement is taken with the device in a magnetic field, *B*, perpendicular to the hole layer plane and intensity $B = 5$ T. The application of an out-of-plane magnetic field is expected to increase the QD confinement and improve the decoupling from the leads, which in GaAs pumps usually results in quantization enhancement [28]. In a typical single-drive tunable-barrier pump the quantized plateau boundaries are set by insufficient loading or incomplete emission and form a checkers-type diagram with trapeze-shaped tiles at fixed values of $\langle n \rangle$ [20]. By contrast, the data presented here show that the regions of quantized current are nested one into another. This becomes clearer by looking at the pumped current derivatives shown in figures 4(d)–(f). The red construction lines highlight the boundaries of each plateau region and reveal significant overlaps between trapezes of different areas and orientation with respect to the gate space. This may suggest that multiple pumps are at work in this device, with each pump producing only a plateau at $\langle n \rangle = 1$. As observed in figure 2, this could be due to the fact that the QD is only able to capture one hole in the experimental conditions we have probed. By taking the Cartesian coordinates of the vertices of each trapeze, one can obtain their areas by simple geometric construction, as shown in figures 4(g)–(i). A Boolean function is used to select regions of the 2D map space where the trapeze areas overlap and to assign different colors depending on how many overlaps are detected. Assuming that each trapeze sets the boundary for a different $\langle n \rangle = 1$ plateau (magenta), the overlap of two trapezes would lead to a region of the map representative of $\langle n \rangle = 2$ (purple), and similarly, three overlapping trapezes would lead to $\langle n \rangle = 3$ (green). Comparing like-for-like panels in the bottom and top row of figure 4, one may find enough similarities to indicate that multiple pumps operating in parallel could be the origin of the nested plateaux observed in the experiments. Finally, note that the observation of an additional plateau in the presence of magnetic field is compatible with the enhancement of current quantisation generated by a parasitic dot that in the absence of such field would not produce a sizable pumped current due to insufficient confinement.

4. Discussion

These experiments have been impacted by the frequent charge fluctuations in the device. The main limitation is that the effect of systematic changes in experimental parameters become intertwined with the effects of random charge rearrangements.
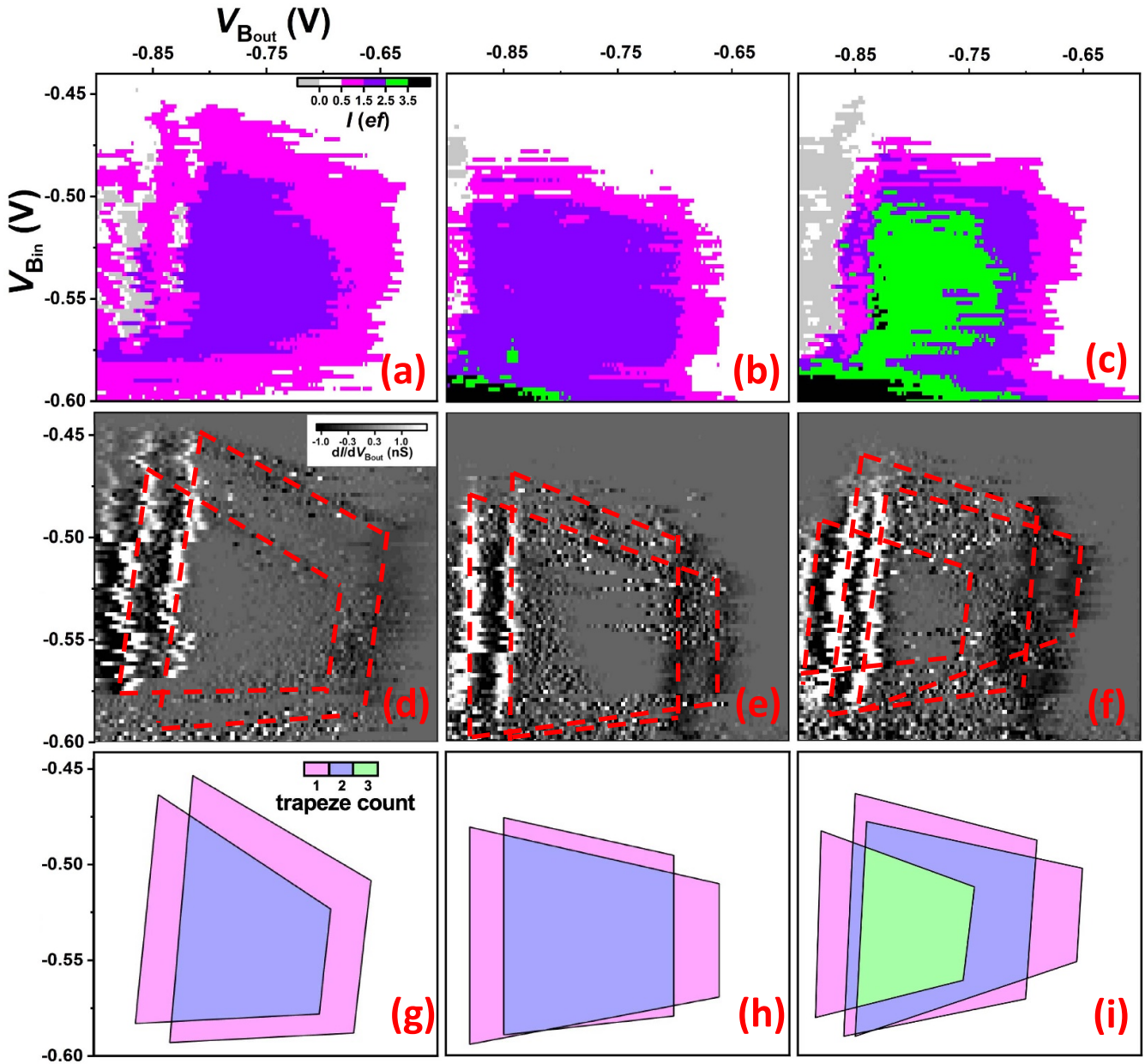
J. Phys. D: Appl. Phys. **54** (2021) 434001

A Rossi *et al*

Figure 4. Pumped current as a function of entrance and exit barrier gate voltages at $f = 100$ MHz, $V_{pp} = 0.275$ V, (a) $V_{PL} = -1.44$ V and $B = 0$ T, (b) $V_{PL} = -1.42$ V and $B = 0$ T, (c) $V_{PL} = -1.42$ V and $B = 5$ T. Scale bar is the same for these three panels. (d) (e) (f) Derivative with respect to V_{Bout} of data in (a), (b) and (c), respectively. Scale bar is the same for these three panels. Red dashed lines are guides to the eye to highlight plateau boundaries. (g), (h) and (i) Geometric trapezes drawn from the construction lines in (d), (e) and (f), respectively. A Boolean function is used to identify regions where trapeze areas overlap and assign different colors: magenta for no overlap, purple for overlap of two trapezes, green for overlap of three trapezes. Voltage ranges on x and y axis are the same for all nine panels.

Distinguishing with confidence between them is not always possible. Besides the instantaneous change of current levels that resulted in noisy pump maps, one has to account for a longer term instability caused by the accumulation in time of multiple random events. This becomes clear if one compares figures 3(a) and 4(b). These two maps are taken at the same experimental conditions (i.e. same drive frequency, amplitude, B-field and V_{PL} values) and yet the pumping regions appear radically different. This is likely

due to the fact that the measurements had been taken few days apart.

It is, therefore, out of an abundance of caution that we do not comment on the theoretical error rate of the pump, which one could have calculated based on the thermal fit value at the inflection point of the plateau [3, 23]. Given that the plateau stability is affected by the fluctuators, it would be misleading to present such information for an isolated stable trace.

In the absence of the random instabilities, one could have also tried to shed more light on the reasons for the capturing of just one hole in the QD and the origin of the multiple pumping mechanisms shown in figure 4. For example, by systematically investigating pump maps as a function of magnetic and electrostatic confinements, one could have gathered relevant information on whether they originated from atomic-like trap states or parasitic QDs, depending on the effect on the plateau length and boundary.

Finally, note that similar devices to those used in this work have resulted to be excellent hosts for spin-based quantum bits [19]. In that case, stable charge configurations have been obtained by reducing gate voltage swings down to few mV. Unfortunately, this strategy does not lend itself effectively to pumping experiments where large sinusoidal drives are typically needed and extensive dc voltage scans have to be carried out to verify the robustness of the transfer protocol [29].

5. Conclusion

In summary, we demonstrated a prototype of single-hole pump in a Ge-based QD. By fitting the current staircase to theoretical models, we conclude that the pump operates in a thermal regime. We observed unusual quantized plateaux boundaries in the 2D pump maps and attributed them to unintended parallel pump operation. More in depth analysis around the theoretical pump error rate, as well as the possible origin of the spurious pumping mechanisms was prevented by device instability in the form of random charge fluctuations.

In the future, these pumps may become useful for metrological applications by contributing to high-accuracy current generation or universality tests. Furthermore, hole pumps in high-mobility Ge could be of interest for the nascent field of fermionic quantum optics [30], as well as for the realisation of single-photon sources based on charge transfer [31]. However, to fulfill these expectations, it will be imperative to improve their charge stability. Recent studies [32, 33] have shown that quieter QDs can be realised when the Ge quantum well is positioned deeper in the heterostructure stack as a result of a thicker (55 nm) $Si_{0.2}Ge_{0.8}$ barrier layer. This also suggests that a possible origin of charge fluctuations resides in trap states at the interface between the Si capping layer and the barrier layer. We expect that the next generation of Ge pumps will directly benefit from this improvement in the fabrication process and will likely achieve much reduced levels of charge fluctuations.

Data availability statement

The data that support the findings of this study are available upon reasonable request from the authors.

ORCID iDs

Alessandro Rossi ⬥ https://orcid.org/0000-0001-7935-7560
Giordano Scappucci ⬥ https://orcid.org/0000-0003-2512-0079
Masaya Kataoka ⬥ https://orcid.org/0000-0001-5780-6871

References

[1] Pekola J P, Saira O-P, Maisi V F, Kemppinen A, Möttönen M, Pashkin Y A and Averin D V 2013 Single-electron current sources: toward a refined definition of the ampere *Rev. Mod. Phys.* **85** 1421

[2] Scherer H and Schumacher H W 2019 Single-electron pumps and quantum current metrology in the Revised SI *Ann. Phys., Lpz.* **531** 1800371

[3] Zhao R, Rossi A, Giblin S P, Fletcher J D, Hudson F E, Möttönen M, Kataoka M and Dzurak A S 2017 Thermal-error regime in high-accuracy gigahertz single-electron pumping *Phys. Rev. Appl.* **8** 044021

[4] Giblin S P, Fujiwara A, Yamahata G, Bae M-H, Kim N, Rossi A, Möttönen M and Kataoka M 2019 Evidence for universality of tunable-barrier electron pumps *Metrologia* **56** 044004

[5] Yamahata G, Giblin S P, Kataoka M, Karasawa T and Fujiwara A 2016 Gigahertz single-electron pumping in silicon with an accuracy better than 9.2 parts in 107 *Appl. Phys. Lett.* **109** 013101

[6] Stein F *et al* 2015 Validation of a quantized-current source with 0.2 ppm uncertainty *Appl. Phys. Lett.* **107** 103501

[7] Scherer H and Camarota B 2012 Quantum metrology triangle experiments: a status review *Meas. Sci. Technol.* **23** 124010

[8] Jeckelmann B, Jeanneret B and Inglis D 1997 High-precision measurements of the quantized hall resistance: experimental conditions for universality *Phys. Rev.* B **55** 13124

[9] Janssen T J B M, Williams J M, Fletcher N E, Goebel R, Tzalenchuk A, Yakimova R, Lara-Avila S, Kubatkin S and Fal'ko V I 2012 Precision comparison of the quantum Hall effect in graphene and gallium arsenide *Metrologia* **49** 294

[10] Niskanen A O, Kivioja J M, Seppä H and Pekola J P 2005 Evidence of cooper-pair pumping with combined flux and voltage control *Phys. Rev.* B **71** 012513

[11] Vartiainen J J, Möttönen M, Pekola J P and Kemppinen A 2007 Nanoampere pumping of cooper pairs *Appl. Phys. Lett.* **90** 082102

[12] Pothier H, Lafarge P, Urbina C, Esteve D and Devoret M H 1992 Single-electron pump based on charging effects *Europhys. Lett.* **17** 249

[13] Pekola J P, Vartiainen J J, Möttönen M, Saira O-P, Meschke M and Averin D V 2008 Hybrid single-electron transistor as a source of quantized electric current *Nat. Phys.* **4** 120

[14] Tettamanzi G C, Wacquez R and Rogge S 2014 Charge pumping through a single donor atom *New J. Phys.* **16** 063036

[15] Roche B, Riwar R P, Voisin B, Dupont-Ferrier E, Wacquez R, Vinet M, Sanquer M, Splettstoesser J and Jehl X 2013 A two-atom electron pump *Nat. Commun.* **4** 1581

[16] Connolly M R *et al* 2013 Gigahertz quantized charge pumping in graphene quantum dots *Nat. Nanotechnol.* **8** 417

[17] Sammak A *et al* 2019 Shallow and undoped germanium quantum wells: a playground for spin and hybrid quantum technology *Adv. Funct. Mater.* **29** 1807613

[18] Lodari M, Tosato A, Sabbagh D, Schubert M A, Capellini G, Sammak A, Veldhorst M and Scappucci G 2019 Light effective hole mass in undoped Ge/SiGe quantum wells *Phys. Rev.* B **100** 041304

[19] Hendrickx N W, Lawrie W I L, Petit L, Sammak A, Scappucci G and Veldhorst M 2020 A single-hole spin qubit *Nat. Commun.* **11** 3478

[20] Kaestner B and Kashcheyevs V 2015 Non-adiabatic quantized charge pumping with tunable-barrier quantum dots: a review of current progress *Rep. Prog. Phys.* **78** 103901

[21] van der Wiel W G, De Franceschi S, Elzerman J M, Fujisawa T, Tarucha S and Kouwenhoven L P 2002 Electron transport through double quantum dots *Rev. Mod. Phys.* **75** 1

[22] Kashcheyevs V and Kaestner B 2010 Universal decay cascade model for dynamic quantum dot initialization *Phys. Rev. Lett.* **104** 186805

[23] Yamahata G, Karasawa T and Fujiwara A 2015 Gigahertz single-hole transfer in Si tunable-barrier pumps *Appl. Phys. Lett.* **106** 023112

[24] Yamahata G, Nishiguchi K and Fujiwara A 2014a Accuracy evaluation and mechanism crossover of single-electron transfer in Si tunable-barrier turnstiles *Phys. Rev.* B **89** 165302

[25] Rossi A *et al* 2014 An accurate single-electron pump based on a highly tunable silicon quantum dot *Nano Lett.* **14** 3405

[26] Yamahata G, Nishiguchi K and Fujiwara A 2014 Gigahertz single-trap electron pumps in silicon *Nat. Commun.* **5** 5038

[27] Rossi A, Klochan J, Timoshenko J, Hudson F E, Möttönen M, Rogge S, Dzurak A S, Kashcheyevs V and Tettamanzi G C 2018 Gigahertz single-electron pumping mediated by parasitic states *Nano Lett.* **18** 4141

[28] Fletcher J D *et al* 2012 Stabilization of single-electron pumps by high magnetic fields *Phys. Rev.* B **86** 155311

[29] Giblin S P, Bae M-H, Kim N, Ahn Y-H and Kataoka M 2017 Robust operation of a GaAs tunable barrier electron pump *Metrologia* **54** 299

[30] Bocquillon E, Freulon V, Berroir J-M, Degiovanni P, Plaçais B, Cavanna A, Jin Y and Fève G 2013 Coherence and indistinguishability of single electrons emitted by independent sources *Science* **339** 1054

[31] Imamoglu A and Yamamoto Y 1994 Turnstile device for heralded single photons: coulombblockade of electron and hole tunneling in quantum confined p-i-n heterojunctions *Phys. Rev. Lett.* **72** 210

[32] Lodari M, Hendrickx N W, Lawrie W I L, Hsiao T-K, Vandersypen L M K, Sammak A, Veldhorst M and Scappucci G 2021 Low percolation density and charge noise with holes in germanium *Mater. Quantum Technol.* **1** 011002

[33] Hendrickx N W, Lawrie W I L, Russ M, van Riggelen F, de Snoo S L, Schouten R N, Sammak A, Scappucci G and Veldhorst M 2021 A four-qubit germanium quantum processor *Nature* **591** 580